Journal of Biomedical Optics

BiomedicalOptics.SPIEDigitalLibrary.org

Line-scanning confocal microscopy for high-resolution imaging of upconverting rare-earth-based contrast agents

Laura M. Higgins
Margot Zevon
Vidya Ganapathy
Yang Sheng
Mei Chee Tan
Richard E. Riman
Charles M. Roth
Prabhas V. Moghe
Mark C. Pierce

SPIE.

Line-scanning confocal microscopy for high-resolution imaging of upconverting rare-earth-based contrast agents

Laura M. Higgins,[a] Margot Zevon,[a] Vidya Ganapathy,[a] Yang Sheng,[b] Mei Chee Tan,[b] Richard E. Riman,[c] Charles M. Roth,[a,d] Prabhas V. Moghe,[a,d] and Mark C. Pierce[a,*]

[a]Rutgers University, Department of Biomedical Engineering, 599 Taylor Road, Piscataway, New Jersey 08854, United States
[b]Singapore University of Technology and Design, Engineering Product Development, 8 Somapah Road 487372, Singapore
[c]Rutgers University, Department of Materials Science and Engineering, 607 Taylor Road, Piscataway, New Jersey 08854, United States
[d]Rutgers University, Department of Chemical and Biochemical Engineering, 98 Brett Road, Piscataway, New Jersey 08854, United States

Abstract. Rare-earth (RE) doped nanocomposites emit visible luminescence when illuminated with continuous wave near-infrared light, making them appealing candidates for use as contrast agents in biomedical imaging. However, the emission lifetime of these materials is much longer than the pixel dwell times used in scanning intravital microscopy. To overcome this limitation, we have developed a line-scanning confocal microscope for high-resolution, optically sectioned imaging of samples labeled with RE-based nanomaterials. Instrument performance is quantified using calibrated test objects. $NaYF_4$: Er, Yb nanocomposites are imaged *in vitro*, and in *ex vivo* tissue specimens, with direct comparison to point-scanning confocal microscopy. We demonstrate that the extended pixel dwell time of line-scanning confocal microscopy enables subcellular-level imaging of these nanomaterials while maintaining optical sectioning. The line-scanning approach thus enables microscopic imaging of this emerging class of contrast agents for preclinical studies, with the potential to be adapted for real-time *in vivo* imaging in the clinic. [DOI: 10.1117/1.JBO.20.11.110506]

Keywords: confocal microscopy; contrast agents; nanomaterials; lanthanides; upconversion.

Paper 150550LR received Aug. 17, 2015; accepted for publication Nov. 2, 2015; published online Nov. 25, 2015.

Nanocomposites containing rare-earth (RE) ions have appealing properties for use as biomedical imaging contrast agents.[1–4] When excited with near-infrared (NIR) light, several of the lanthanide elements, including erbium, thulium, and holmium, emit photons at visible wavelengths through energy transfer upconversion (ETU) processes. This avoids excitation at visible or ultraviolet wavelengths, which generates unwanted autofluorescence and limits penetration depth in tissue. The upconversion of NIR photons to visible emission wavelengths can be achieved with continuous wave (CW) excitation sources, in contrast to the femtosecond pulsed lasers required for multiphoton imaging. RE ions can also be rendered biocompatible and functionalized with targeting ligands for molecular imaging.[3]

Whereas RE nanocomposites have been used for macroscopic imaging in preclinical animal models, the long emission lifetimes of RE ions have limited their use in high-resolution imaging. Although the nonlinear ETU processes can theoretically provide inherent optical sectioning, the high excitation power required for real-time imaging saturates the two-photon processes.[5] This shifts the quadratic relationship between excitation power and emission intensity toward a linear relationship, requiring additional means for sectioning, such as point-scanning confocal or multiphoton microscopy.[5–7] These imaging methods sweep a diffraction-limited excitation spot across the specimen in two dimensions, resulting in very short pixel dwell times (~100 ns) if real-time image frame rates are required. RE emission lifetimes are typically on the order of several milliseconds, compared to nanoseconds for conventional organic fluorophores.[8,9] The large discrepancy between pixel dwell time and emission lifetime results in the collection of light from sample regions that were excited several milliseconds earlier. This leads to the appearance of a smearing effect, where punctate sources of upconversion intensity appear spatially spread along the direction of the fast scan.

Previous attempts to provide cellular-level imaging of REs have included point-scanning confocal microscopy, where the detection pinhole prevents collection of light from time points beyond the pixel dwell time.[6,10] Although a small pinhole can reduce unwanted smearing, only a small fraction of the RE's emission is collected. Deconvolution methods have also been applied to remove the long-lived emission intensity contributions from the captured image.[7] This computational approach has been shown to work well for thin, sparsely labeled specimens, but may be challenging to implement in real time, in thick tissues, or in homogeneously labeled regions. Imaging upconversion light with a two-dimensional CCD camera enables the pixel dwell time to be lengthened beyond the RE emission lifetime,[6,11] but this full-field approach cannot easily translate to intravital microscopy in thick tissues where optical sectioning is required to eliminate out-of-focus light.

In contrast to point-scanning and full-field approaches, line-scanning confocal microscopy excites and collects light from all points along a one-dimensional line in parallel. A focused line of excitation light is swept across the sample in the direction perpendicular to the length of the line. By exciting and collecting light from all points along the line simultaneously, the pixel dwell time is longer than point scanning by a factor equal to the number of points within the line (e.g., 500 to 1000). The line-scanning architecture has been used to create very fast confocal imaging platforms,[12] and its relative simplicity has led to the design of compact instruments for clinical applications.[13–16] Here, we develop and use line-scanning confocal microscopy in a new context, to address the problem of long emission

*Address all correspondence to: Mark C. Pierce, E-mail: mark.pierce@rutgers.edu

1083-3668/2015/$25.00 © 2015 SPIE

lifetimes in RE-based upconverting contrast agents. The pixel dwell time is made comparable to the RE ions' lifetime, and real-time imaging with optical sectioning ability is conserved.

RE-doped nanoparticles were synthesized using the solvothermal decomposition method described previously.[17] The resulting $NaYF_4$:Er, Yb nanoparticles (~9 to 11 nm in diameter) were encapsulated in human serum albumin, forming RE albumin nanocomposites (REANCs), each ~100 nm in diameter and containing ~30 individual RE nanoparticles.[18]

Under CW excitation at 980 nm, the $NaYF_4$:Er, Yb nanoparticles' upconversion was measured using a fiber-coupled spectrometer (Ocean Optics, USB4000-VIS-NIR-ES). The emission lifetime was measured at 540 and 650 nm using the visible single photon counting photomultiplier module (Hamamatsu R928P) on an Edinburgh Instruments FLS980 spectrometer, following excitation with an electronically modulated (10 μs) 980 nm source.

To assemble the line-scanning confocal upconversion microscope, the output from a single-mode fiber-coupled diode laser with 980 nm wavelength (QPhotonics) was first collimated to a circular beam diameter of 8.0 mm ($1/e^2$) before being focused by a 150-mm focal length achromatic cylindrical lens (Thorlabs) [Fig. 1(a)]. The resulting line focus is oriented parallel to the y axis in Fig. 1(a) and positioned at the back aperture of a microscope objective. 20×/0.40 (Olympus Plan N), 40×/0.75 (Olympus UPlan FLN), and 100×/1.30 (Nikon Plan Fluor) objective lenses provided varying fields of view and resolution. A single-axis galvanometer scanner is located as close as possible to the objective back aperture (a distance of 20 mm) and pivots about the x axis in Fig. 1(a). The visible upconversion light returning from the specimen is transmitted through a short-pass dichroic mirror (Thorlabs DMSP805), transmitted by a 519 to 700 nm band-pass filter (Semrock), and focused by a 200-mm focal length achromat lens onto a line-scan camera (e2v, Aviiva EM1) with 1024 pixels, each 14 μm wide and 28 μm tall and oriented parallel to the x axis in Fig. 1(a). Data from the camera are acquired over the GigE bus at 1000 lines/s and synchronized with the galvanometer in LabVIEW to generate 1024×512 pixel images at 1.9 frames/s. The signals measured at adjacent pixels along the pixel array are averaged to generate 512×512 pixel images.

The field of view was measured for each objective lens by imaging a calibrated grid target (Thorlabs). Images were digitally cropped to the region where the intensity measured from a uniform target was at least $1/e^2$ of the maximum level. A high-resolution USAF 1951 target (Edmund Optics) was imaged to evaluate lateral resolution for the 20×/0.40 objective. For the higher numerical aperture (NA) objectives, the microscope resolved all nine groups on the target, so the full width at half maximum (FWHM) of the derivative of an intensity profile across a lateral edge was measured to quantify lateral resolution. Optical sectioning was determined by acquiring a sequence of images as a mirror was translated through the focus and measuring the mean pixel value over the central region of these images. No additional confocal slit aperture was used; the camera's nominal pixel height (28 μm) was equivalent to 0.76 Airy units, defined as $1.22\lambda/\mathrm{NA}$.

To assess the performance of line-scanning confocal microscopy for imaging RE-based contrast agents, clusters of $NaYF_4$:Yb, Er nanoparticles were deposited on a microscope slide and excited with a power of 14.0 mW (distributed over the length of the line focus). For *in vitro* studies, MDA-MB-231 human breast cancer cells cultured in Dulbecco's modified Eagle medium supplemented with 10% fetal bovine serum and 1% Penicillin/streptomycin were plated on Lab-Tek II chambered glass slides at a density of 15,000 cells/well and allowed to adhere for 24 h. Cells were then treated with 10% v/v REANCs for 24 h before being washed, fixed, and counterstained with proflavine to highlight cell nuclei. Under a protocol approved by Rutgers University IACUC, athymic nude mice were inoculated with either MDA-MB-231 or 4175-TR human breast cancer cells on the dorsal flanks. Once subcutaneous tumors were established, REANCs were administered via tail vein injection. After eight weeks, animals were euthanized and xenograft tumors and livers were excised and flash frozen, with 60-μm thick tissue cryosections mounted and coverslipped on microscope slides. Cells and tissues were imaged with line illumination of 93.3 and 168.2 mW power at the sample, respectively.

A separate point-scanning confocal microscope was built to image the RE samples using the same excitation source, emission filter, and objective lens as the line-scanning system. A pair of galvanometer scanners (Cambridge Technology 6210) swept the incident spot over the sample in two dimensions. A photomultiplier tube (Hamamatsu R3896) served as the detector in the point-scanning system, which acquired 480×460 pixel images, covering a 550×530 μm^2 field of view ($1/e^2$) at 2 frames/s. A commercial point-scanning confocal platform (Leica TCS

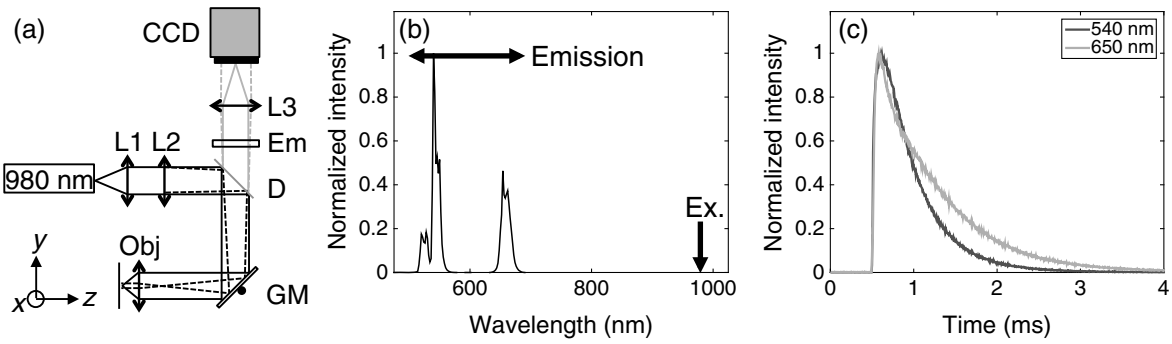

Fig. 1 (a) Schematic layout of the line-scanning confocal microscope. L1, collimating lens; L2, cylindrical lens; L3, detector lens; D, dichroic mirror; Em, emission filter; GM, scanning galvanometer-mounted mirror; Obj, objective lens. (b) Upconversion emission spectrum and (c) temporal emission intensity at 540 (black) and 650 nm (gray) measured for $NaYF_4$:Er, Yb nanoparticles under 980 nm excitation. The calculated decay times for the 540 and 650 nm emission are 460 and 750 μs, respectively.

SPII) was used with 488 nm excitation to image autofluorescence from the REANCs albumin shell and confirm the source of the upconversion signal observed under line-scanning confocal microscopy.

Figure 1(b) demonstrates the upconversion emission spectrum measured from $NaYF_4$:Er, Yb nanoparticles under CW illumination at 980 nm, with green (515 and 541 nm) and red (650 nm) light arising from electronic transitions in erbium ions.[19] Figure 1(c) shows the typical decay curves for $NaYF_4$:Er, Yb spanning several milliseconds.

With the 20× /0.40 objective, the field of view of the line-scanning confocal microscope [xy plane in Fig. 1(a)] was measured to be 570×400 μm^2 ($1/e^2$). Group 8 element 5 of a 1951 USAF resolution target was imaged with 29% contrast, corresponding to a lateral resolution of 2.5 μm [Figs. 2(a) and 2(b)]. Optical sectioning was measured to be 9.3 μm (FWHM) [Fig. 2(c)]. The theoretical lateral resolution and optical sectioning were 1.6 and 6.6 μm, respectively.[20] The fields of view for the 40× /0.75 and 100× /1.30 objectives were measured to be 260×170 μm^2 ($1/e^2$) and 100×50 μm^2 ($1/e^2$), respectively. Theoretical and experimental lateral resolution and optical sectioning values are summarized for each objective lens in Table 1.

Figure 3 demonstrates line-scanning reflectance [Fig. 3(a)] and line-scanning upconversion [Fig. 3(b)] confocal imaging of RE-doped nanoparticles. With the 20× /0.40 objective lens, clusters of particles generate a clear, high-contrast upconversion image [Fig. 3(b)]. When imaged using the custom-built point-scanning confocal microscope with no pinhole [Fig. 3(d)], the characteristic smearing of the upconversion can be observed in the direction of the fast scan. The addition of a 100-μm pinhole reduced this effect [Fig. 3(e)], but, with a diameter of 5.4 Airy units, provided only weak optical sectioning. Reducing the point-scanning confocal pinhole to 25 μm (1.3 Airy units) provided an optical sectioning strength comparable to the line-scanning microscope [Fig. 3(b)],[21] and also significantly reduced the signal-to-background level [Fig. 3(f)].

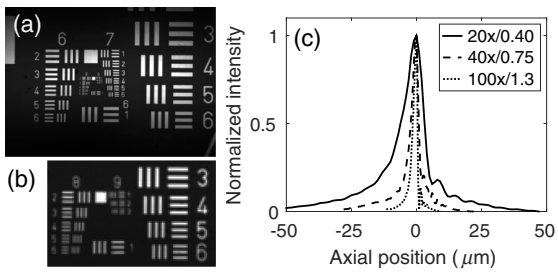

Fig. 2 (a) and (b) High-resolution USAF 1951 target (20× /0.40 objective). (c) Axial response to a mirror scanned through the focus of three objective lenses.

Table 1 Lateral resolution and optical sectioning strength for the line-scanning confocal microscope using different objective lenses.

	Lateral (μm)		Sectioning (μm)	
	Theory	Meas.	Theory	Meas.
20 × /0.40	1.6	2.5	6.6	9.3
40 × /0.75	0.8	1.2	1.6	3.0
100 × /1.30	0.3	0.6	0.7	1.8

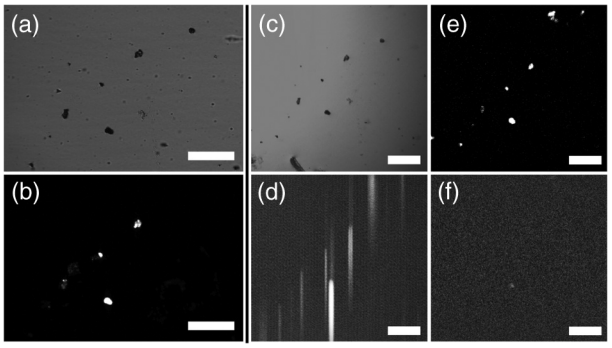

Fig. 3 Confocal microscopy of rare-earth (RE) nanoparticles (20× /0.40 objective): (a) line-scanning reflectance, (b) line-scanning upconversion, (c) point-scanning reflectance, (d) point-scanning upconversion (no pinhole), (e) point-scanning upconversion (100 μm pinhole), and (f) point-scanning upconversion (25 μm pinhole). Scale bars = 100 μm.

Line-scanning confocal microscopy of REANCs is demonstrated in biological samples in Fig. 4. As a negative control, cells without REANCs showed no upconversion signal [Fig. 4(a)]. Following the addition of REANCs, localization of the contrast agent on and within the cells is apparent [Fig. 4(b)].

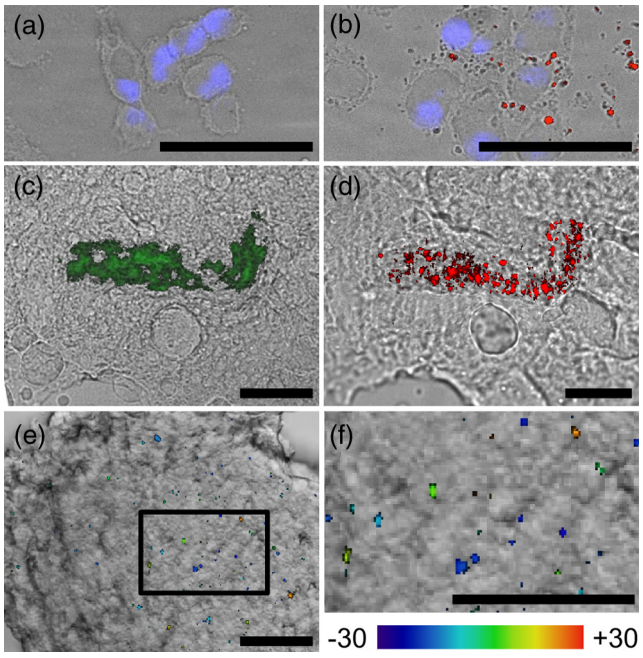

Fig. 4 Line-scanning confocal upconversion microscopy of biological samples. (a) and (b) Proflavine (blue) stained cells *in vitro* (a) without RE albumin nanocomposites (REANCs) and (b) following addition of REANCs, overlaid with the upconversion image (red). Mouse subcutaneous tumor tissue section with (c) point-scanning confocal microscopy of albumin shell autofluorescence overlaid (green) and (d) line-scanning confocal microscopy of the same section as in (c) with upconversion image overlaid (red). Video 1 shows corresponding z-stack with 1 μm step size. (e) Mouse liver section with z-stack projection of upconversion image overlaid. (f) Selected region from (e) magnified at 2.5× shows upconversion from REs at depths ranging from −30 to +30 μm. Scale bars = 50 μm. (Video 1, MP4, 239 kB [URL: http://dx.doi.org/10.1117/1.JBO.20.11.110506.1]).

Figure 4(c) shows point-scanning confocal microscopy of mouse tumor tissue at 40×. RE signal was not detectable on the commercial system, but the albumin shell autofluorescence was detected under 488 nm excitation to establish the location of REANCs (green overlay). Under line-scanning microscopy [Fig. 4(d)], the upconversion light could be readily detected (red overlay), coincident with the albumin shell signal. The corresponding video clip shows a z-stack sequence of upconversion images as the specimen is translated through the focus at 1 μm steps (Video 1), demonstrating the ability of the line-scanning microscope to acquire optically sectioned images without smearing of the RE emission. Figure 4(e) shows a projection of the RE signal overlaid with a white-light image of *ex vivo* liver tissue, which takes up the REANCs due to the hepatic clearance pathway. The highlighted region in Fig. 4(e) is displayed in Fig. 4(f) at 2.5× magnification to show more detailed REANC localization. The colormap represents the z-position of the particles in the tissue at depths ranging from −30 to +30 μm.

REANC-based contrast agents have appealing properties for targeted imaging of disease. These materials have been functionalized with targeting ligands against established biomarkers for neoplastic lesions.[3] NIR excitation allows for deeper imaging than with visible fluorophores, whereas reduced autofluorescence can improve signal-to-background levels. The ETU process involves real energy levels, allowing for use of low-intensity CW excitation sources, in contrast to the complex and expensive ultrafast lasers required for multiphoton techniques.

Although preclinical *in vivo* imaging studies have demonstrated these benefits at the macroscopic scale, the long emission lifetimes of RE ions have hindered efforts to enable cellular-level imaging with these contrast agents. The pinhole in confocal microscopy prevents collection of RE emissions occurring beyond the pixel dwell time, but drastically reduces light collection efficiency and compromises the ability to image beneath the tissue surface. Nonlinear microscopy techniques that use nondescanned detection also suffer from smearing of the RE emission along the fast-scan axis due to the long emission lifetime relative to the pixel dwell time.

We have shown here that line-scanning confocal upconversion microscopy provides a solution to the unique challenges posed by high-resolution imaging of RE-based nanomaterials. Previous researchers have established the feasibility of implementing line-scanning methods in clinically viable devices.[14,16,22] We anticipate that the line-scanning approach will assist in translation of this class of optical contrast agent toward clinical studies and permit microscopic scale visualization of RE uptake alongside existing macroscopic imaging platforms.

Acknowledgments

This work was supported by the National Institutes of Health under grant R01 EB018378.

References

1. S. F. Lim et al., "In vivo and scanning electron microscopy imaging of upconverting nanophosphors in Caenorhabditis elegans," *Nano Lett.* **6**(2), 169–174 (2006).
2. G. Wang, Q. Peng, and Y. Li, "Upconversion luminescence of monodisperse $CaF_2:Yb^{3+}/Er^{3+}$ nanocrystals," *J. Am. Chem. Soc.* **131**(40), 14200–14201 (2009).
3. D. J. Naczynski et al., "Rare-earth-doped biological composites as in vivo shortwave infrared reporters," *Nat. Commun.* **4**, 2199 (2013).
4. Q. Q. Dou, H. C. Guo, and E. Ye, "Near-infrared upconversion nanoparticles for bio-applications," *Mater. Sci. Eng. C* **45**, 635–643 (2014).
5. M. Pollnau et al., "Power dependence of upconversion luminescence in lanthanide and transition-metal-ion systems," *Phys. Rev. B* **61**(5), 3337 (2000).
6. J. Pichaandi et al., "Two-photon upconversion laser (scanning and wide-field) microscopy using Ln^{3+}-doped $NaYF_4$ upconverting nanocrystals: a critical evaluation of their performance and potential in bioimaging," *J. Phys. Chem. C* **115**(39), 19054–19064 (2011).
7. C. F. Gainer, U. Utzinger, and M. Romanowski, "Scanning two-photon microscopy with upconverting lanthanide nanoparticles via Richardson-Lucy deconvolution," *J. Biomed. Opt.* **17**(7), 076003 (2012).
8. J. R. Lakowicz, "Radiative decay engineering: biophysical and biomedical applications," *Anal. Biochem.* **298**(1), 1–24 (2001).
9. D. Yuan et al., "Comprehensive study on the size effects of the optical properties of $NaYF_4:Yb,Er$ nanocrystals," *J. Phys. Chem. C* **117**(25), 13297–13304 (2013).
10. M. Yu et al., "Laser scanning up-conversion luminescence microscopy for imaging cells labeled with rare-earth nanophosphors," *Anal. Chem.* **81**(3), 930–935 (2009).
11. E. A. Grebenik et al., "Feasibility study of the optical imaging of a breast cancer lesion labeled with upconversion nanoparticle biocomplexes," *J. Biomed. Opt.* **18**(7), 076004 (2013).
12. R. Wolleschensky, B. Zimmermann, and M. Kempe, "High-speed confocal fluorescence imaging with a novel line scanning microscope," *J. Biomed. Opt.* **11**(6), 064011 (2006).
13. Y. S. Sabharwal et al., "Slit-scanning confocal microendoscope for high-resolution in vivo imaging," *Appl. Opt.* **38**(34), 7133–7144 (1999).
14. A. A. Tanbakuchi et al., "Clinical confocal microlaparoscope for real-time in vivo optical biopsies," *J. Biomed. Opt.* **14**(4), 044030 (2009).
15. P. J. Dwyer, C. A. DiMarzio, and M. Rajadhyaksha, "Confocal theta line-scanning microscope for imaging human tissues," *Appl. Opt.* **46**(10), 1843–1851 (2007).
16. B. Larson, S. Abeytunge, and M. Rajadhyaksha, "Performance of full-pupil line-scanning reflectance confocal microscopy in human skin and oral mucosa in vivo," *Biomed. Opt. Express* **2**(7), 2055–2067 (2011).
17. G.-S. Yi and G.-M. Chow, "Water-soluble $NaYF_4:Yb,Er(Tm)/NaYF_4$/polymer core/shell/shell nanoparticles with significant enhancement of upconversion fluorescence," *Chem. Mater.* **19**(3), 341–343 (2007).
18. D. J. Naczynski et al., "Albumin nanoshell encapsulation of near-infrared-excitable rare-earth nanoparticles enhances biocompatibility and enables targeted cell imaging," *Small* **6**(15), 1631–1640 (2010).
19. J. Suyver et al., "Upconversion spectroscopy and properties of $NaYF_4$ doped with Er^{3+}, Tm^{3+} and/or Yb^{3+}," *J. Lumin.* **117**(1), 1–12 (2006).
20. G. S. Kino and T. R. Corle, *Confocal Scanning Optical Microscopy and Related Imaging Systems*, Academic Press, San Diego, California (1996).
21. T. Wilson and A. Carlini, "Size of the detector in confocal imaging systems," *Opt. Lett.* **12**(4), 227–229 (1987).
22. D. X. Hammer et al., "Line-scanning laser ophthalmoscope," *J. Biomed. Opt.* **11**(4), 041126 (2006).